Kufa Journal of Engineering
Vol. 13, No. 4, October 2022, P.P. 39-52
Article history: Received date: 3 June 2022, accepted date: 14 October 2022

COMPARATIVE THERMAL PERFORMANCE ANALYSIS OF ROOFTOPS WITH ELEVATED CEILING CONFIGURATION

Kamiyo O.M.*[1] and Ekundayo O.E[2].

[1]Department of Mechanical Engineering, University of Lagos, Lagos, Nigeria. Email: okamiyo@unilag.edu.ng

[2]Department of Mechanical Engineering, University of Lagos, Lagos, Nigeria. Email: oekundayo01@gmail.com

***[1]Corresponding author**

HTTPS://DOI.ORG/10.30572/2018/KJE/130404

ABSTRACT

In this study, thermal performance of different pitched roofs with elevated ceiling configuration is analyzed and compared. Three different ceiling shapes, viz., cathedral, barrel-vault and A-frame, at the same pitch angle and ceiling material, under winter heating are examined numerically by solving the steady-state air and heat flow problems simultaneously. In all the roofs, the airflow fields show counter-rotating recirculating cells. The multicellular flow field promotes uniform temperature distribution within the enclosures. Heat loss to the attic from the space below increases with the closeness of the hot ceiling to the cold inclined walls. In the A-frame roof, there is uniform convective heat transfer. But in the cathedral and barrel-vault roofs, near the bottom corners, conductive heat exchange predominates. In all, the thermal performance of the barrel-vault is least while that of the cathedral is best. This observation is useful on the application of insulation when using such ceiling shapes.

KEYWORDS

Ceiling Shape, Rooftops, Natural Convection, Thermal Performance, Heat Transfer.

1. INTRODUCTION

In a building envelope with pitched roof, the attic is often represented by a triangular shape with the inclined walls exposed to solar radiation or snow deposit. The ceiling wall separates the attic space from the occupied space below it. The aerodynamics and thermal loads acting on a ceiling wall vary during the day or night time and during winter or summer season due to the periodic changes in ambient temperatures. These affect the thermal performance of building roofs (Al-Sanea, 2002). In air-conditioning of buildings during winter, to achieve acceptable indoor comfort conditions requires reducing heat losses. In practice, a number of methods are commonly adopted to enhance the thermal performance of building envelopes. These include reducing heat loss to the rooftop by increasing insulation and reducing heat loss through higher thermal mass walls.

Studies on thermal performance of building attics have generated a lot of interests over the years owing to its importance in building engineering. Yilmaz (2007) evaluated various energy efficient design strategies to compare thermal performance of buildings for different climatic zones. Alencastro *et al.* (2018) examined the relationship between quality defects and the thermal performance of buildings. Elnokaly *et al.* (2019) performed parametric investigation of the thermal performance of vaulted roofs exposed to hot-arid climates. Rooftops of pitched roofs are often modelled as two-dimensional triangular cross-section. Heat transfer in such enclosures under summer and winter boundary conditions have been investigated using control parameters such as changes in pitch angle, Rayleigh number and aspect ratio (Koca *et al.*, 2007; Oztop *et al.*, 2007; Varol *et al.*, 2007a, 2007b, Koca *et al.*, 2008, Oztop *et al.*, 2012). Comparing a case of uniform heating within a triangular enclosure to that of non-uniform heating, Kent (2009a, 2009b) observed that the base angle of a symmetrical triangular roof has a drastic influence on the flow field and isotherms. Kamiyo *et al.* (2010) reviewed previous studies on natural convection in triangular enclosures depicting pitched rooftops and concludes its dependence on enclosure geometry, orientation, and thermal boundary conditions.

Zhai *et al.* (2018) numerically investigated sectioned triangular roof and demonstrated that there exist different regimes of transient natural convection on the roof. Cui *et al.* (2019) considered the effect of varying the aspect ratio of another sectioned triangular roof to predict the natural convective heat transfer within it under unsteady condition. Raj *et al.* (2018) performed an experimental study of natural convection inside a vented triangular roof when combined with surface radiation. Recently, analysis of the flow and thermal fields in raised-ceiling and M-shaped roofs heated from the base wall is carried out by Kamiyo (2020; 2021).

In modern times, ceiling shapes are constructed with architectural aesthetics as the main goal. Therefore, different shapes are developed indiscriminately without considering their effect on the thermal performance of the roof. This study focuses on the effect of ceiling shape on the thermal performance of selected three with special features among the universally-used pitch-roof shapes. The ceiling shapes selected are commonly referred to as Cathedral, A-frame and Barrel-vault. The ceiling in each case is made of poly vinyl chloride (PVC) – a synthetic polymer of plastic. Same design parameters are employed for the sake of comparison under the same winter condition.

2. METHODOLOGY

The roof geometries investigated are shown in Fig. 1(a-c). The roof is modelled as a long, horizontal, air-filled attic of isosceles triangular cross-section with the base wall, representing the ceiling having different shapes. For the cathedral roof, Fig. 1(a), the ceiling follows the profile of the rooftop but it's pitched at an angle α (= ½β) which depends on the roof architecture. In Fig. 1(b), the ceiling of the A-frame roof also follows the profile of the rooftop with a gap of 0.125H between them. Barrel-vault roof, on the other hand, has a curved ceiling with height to width ratio of 0.128. Based on the geometry of the roofs, the flow field and heat transfer can be regarded as being two-dimensional (Penot and N'Dame, 1992).

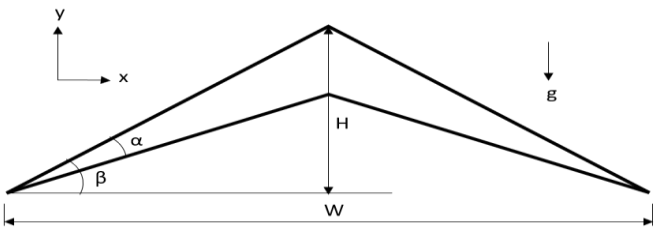

(a) Cathedral roof

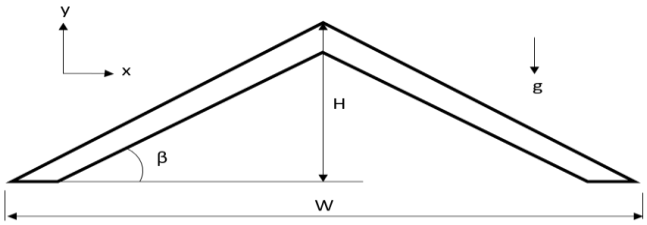

(b) A-frame roof

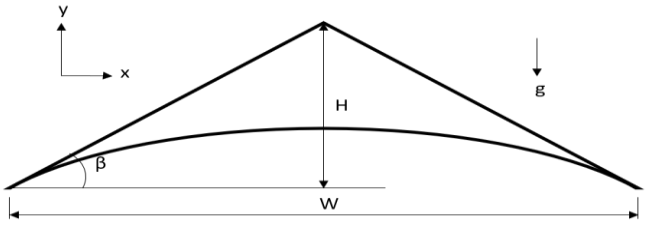

(c) Barrel-vault roof

Fig. 1. Physical models of the roofs.

Using the following dimensionless parameters,

$$X = \frac{x}{H};\ Y = \frac{y}{H};\ U = \frac{uH}{\alpha'};\ V = \frac{vH}{\alpha'};\ \theta = \frac{T-T_C}{T_H-T_C};\ P = \frac{pH^2}{\rho\alpha'^2};\ Ra = \frac{g\beta'\Delta T H^3}{\nu\alpha'};\ Pr = \frac{\nu}{\alpha'}.$$

the non-dimensional forms of the governing equations, with Boussinesq approximation (Ridouane *et al*., 2005), are expressed as:

Conservation of Mass:

$$\frac{\partial U}{\partial X} + \frac{\partial V}{\partial Y} = 0 \tag{1}$$

Conservation of Momentum:

U-momentum

$$U\frac{\partial U}{\partial X} + V\frac{\partial U}{\partial Y} = -\frac{\partial P}{\partial X} + \Pr\left(\frac{\partial^2 U}{\partial X^2} + \frac{\partial^2 U}{\partial Y^2}\right) \tag{2}$$

V-momentum

$$U\frac{\partial V}{\partial X} + V\frac{\partial V}{\partial Y} = -\frac{\partial P}{\partial Y} + \Pr\left(\frac{\partial^2 V}{\partial X^2} + \frac{\partial^2 V}{\partial Y^2}\right) + RaPr\theta \tag{3}$$

Conservation of Energy

$$U\frac{\partial \theta}{\partial X} + V\frac{\partial \theta}{\partial Y} = \left(\frac{\partial^2 \theta}{\partial X^2} + \frac{\partial^2 \theta}{\partial Y^2}\right) \tag{4}$$

In reality, the roof size and environmental thermal conditions vary. Therefore, physical dimensions and the boundary conditions of the computational domain are normalized.

Aspect ratio, Tan β = 2H/W where W = 1. In many cases, in reality, angle β varies. But in this study, 18° is chosen for angle β in each of the three ceiling shapes considered.

The boundary conditions for the computational domains are:

Temperature:

Isothermal hot ceiling: θ = 1.

Isothermal cold inclined walls: θ = 0.

Velocity:

Along the walls, no slip condition applies: U = V = 0

As a result of traditional hearth method of heating in winter, warm air accumulating at the ceiling level heats it to slightly above the room temperature. The upper walls are taken to be covered with snow. The attic is filled with dry air (Pr = 0.71), regarded as a viscous, incompressible, Newtonian fluid, with no internal heat generation. The Rayleigh number for the geometry and boundary conditions results in 7.88×10^7.

Fig. 2. Mesh for the Cathedral roof.

Unstructured tetrahedral mesh with multiples of fine elements was generated for each of the roofs. Fig. 2 shows the mesh generated for the cathedral roof. To test for grid independence and hence the accuracy of the numerical scheme, a number of simulations with varying number of elements for each roof were conducted. The result of the maximum relative velocity, U_{max}, was compared with the number of elements as shown in Table 2 for the cathedral roof

Table 2. Grid independence test for the Cathedral roof.

Number of elements	13,075	42,869	51,758
U_{max}	0.1405	0.1357	0.1351

CFD package, ANSYS FLUENT, was used to solve the coupled partial differential equations (1) to (4) that describe the steady, laminar natural convective heat and fluid flow in the enclosures. As available in the software, spatial discretization of the momentum and energy equations was done with a QUICK scheme. SIMPLE algorithm was adopted to resolve the coupling between pressure and velocity. The equations were solved iteratively. The convergence target used for the continuity equation was 10^{-5} and 10^{-7} was set as target for the momentum and energy equations. Reliance on the effectiveness of ANSYS FLUENT package to adequately simulate the current natural convection in enclosures problem is based, among other publications, on the excellent agreement obtained with the experiment performed by Yesiloz and Aydin (2013) for laminar natural convection in a right-angled triangular enclosure heated from below within the range $10^3 \leq Ra \leq 10^7$ and the numerical results obtained using ANSYS FLUENT for the same configuration.

3. RESULTS AND DISCUSSION

The flow fields in the roofs are analyzed using the results of the streamlines, the relative velocity and the pressure contour plots, and the graphical plots of the values of the relative velocity at the vertical midsection of each roof. The thermal fields are presented using the temperature contour plots and the graphical plots of the temperature variation at the vertical midsection of the roofs. The variation of the local Nusselt number along the hot ceiling and cold inclined walls and the mean Nusselt number for the base ceiling of each roof are collectively used to analyze the thermal performance of the roofs.

3.1 Flowfield

In Fig. 3, airflow streamlines within the roofs indicate multicellular flows similar to the classical Rayleigh-Bernard convection. The formation of the cells is as a result of hot, rarefied fluid rising from the hot ceiling towards the upper cold inclined walls in form of plumes. As a plume strike the upper wall, it bifurcates in either direction; losing its heat content in the process. Each part then flows down in form of a cold jet back to the ceiling where it is reheated to repeat the cycle. As a result, counter-rotating, recirculating cells of different speeds of rotation are formed across the roof. The roof pitch and the length of the upper walls being the same, the shape of the ceiling is found to strongly influence the size and number of cells formed in each roof. The A-Frame roof has twenty-five cells of averagely uniform size and rotational speed. But in the Cathedral roof, there are fourteen cells of varying sizes with different speed of rotation. Barrel-vault roof has twelve cells of varying sizes and speed. This consequently control the utilization of the attic space especially when filled with moist air.

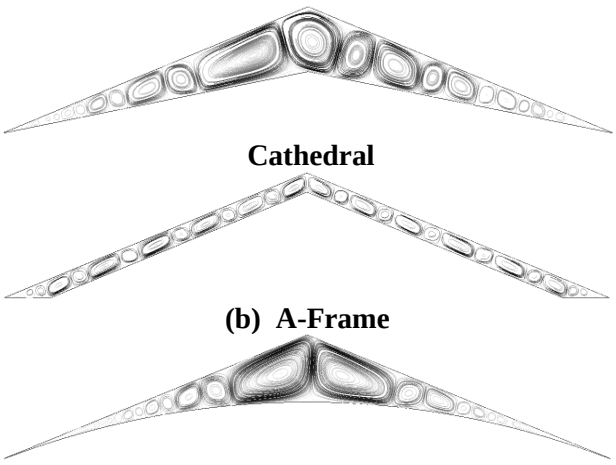

Cathedral

(b) A-Frame

(c) Barrel-vault

Fig. 3. Airflow streamlines within the roofs.

The distribution of the air velocity within the roofs is presented in Fig. 4. Velocity is high at the outer circumference of a cell specifically where counter-rotating cells rub on each other and as they flow along the walls. As in a vortex, the rotating velocity of a cell reduces from the outer circumference towards its core. This is typically the case in the A frame roof where the speed of rotation of a vortex is generally uniform. For the cells in the cathedral and barrel-vault roofs, the circumferential velocity reduces with the size of the cell; from the large cells at the midsection to the bottom corners. Close to the bottom corners, there is virtually no movement of air because conduction dominates there. This stagnant area is smallest in the A-frame roof and largest in the barrel-vault roof.

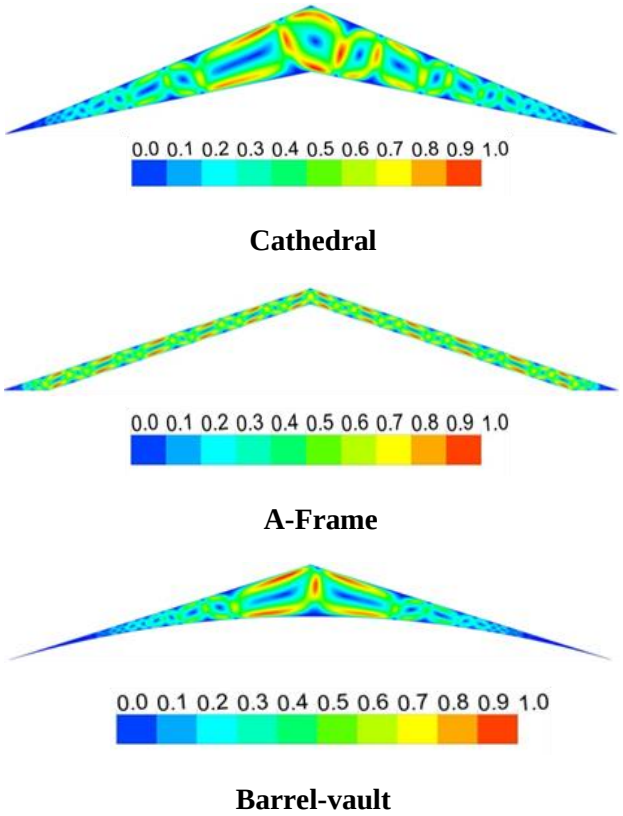

Fig. 4. Air velocity distribution within the roofs.

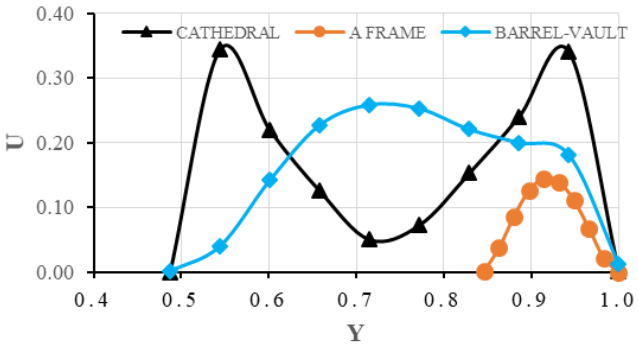

Fig. 5. Air velocity variation along vertical midsections of the roofs.

The midsection of a roof is of interest because of the large space available for storage of sometimes sensitive materials. It is therefore necessary to know the state of moist air movement within the area. The variation of the dimensionless air velocity, U, along the vertical midsection of each roof is shown in Fig. 5. The cross-sectional line goes across the diameter of the largest cell at the midsection of the cathedral roof. Velocity reduces from 0.34 at the outer circumferences to 0.05 at the centre of the cell. Aerodynamic boundary layers of 0.055Y thick form at the lower and upper walls. In the A-frame and barrel-vault roofs, the midsection coincides with the path of a plume. In both cases, with the strong push of the buoyant force, the velocity increases as hot air rises from the ceiling to a peak midway. It reduces towards the upper wall as the plume loses strength while struggling through heavy cold air.

3.2 Pressure distribution

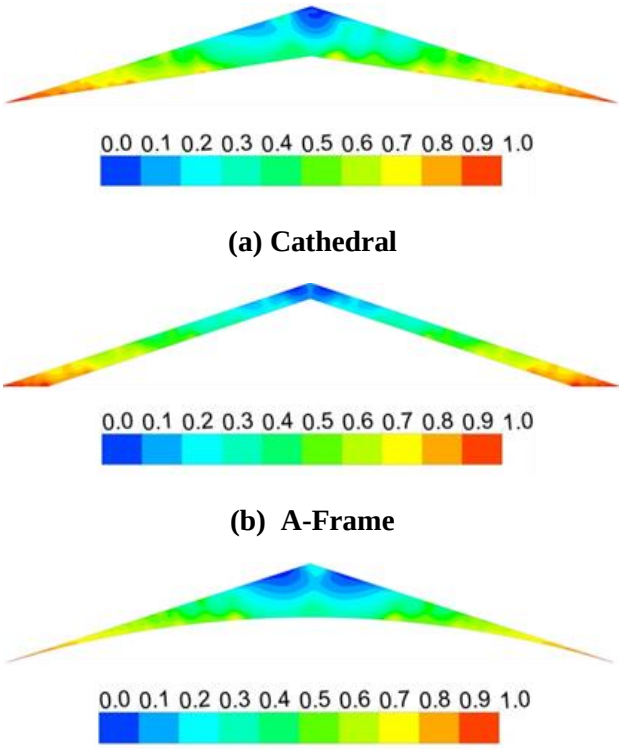

(a) Cathedral

(b) A-Frame

(c) Barrel-vault

Fig. 6. Air pressure distribution within the roofs.

Pressure distribution of air within each roof is shown in Fig. 6 in form of contour plots. In contrast to the air velocity distribution, air pressure is relatively high at the bottom corners where air movement is suppressed by the closeness of the walls while it is very low at the midsection where there is enough room for convection. The upper vertex is particularly noted to be the lowest pressure area. Knowledge of the variation of pressure within the roofs is

important so as to guide the building owners on the placement of the vent openings and items sensitive to pressure variation.

3.3 Temperature distribution

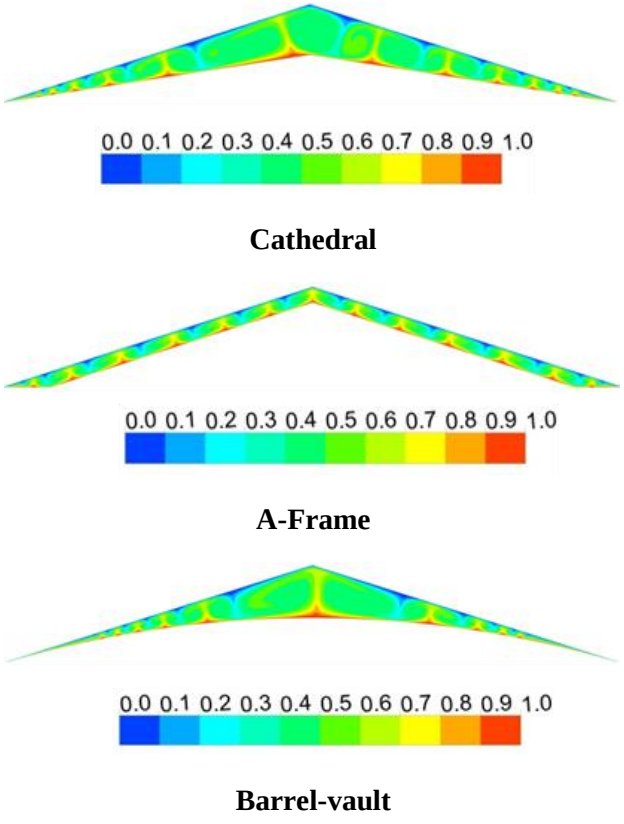

Fig. 7. Temperature distribution within the roofs.

As air along the ceiling is heated, hot air rises under the buoyant force towards the inclined wall in form of plumes. On hitting an upper wall, a plume splits in either direction. As it flows downwards the inclined wall, it loses its heat content and becomes heavier. Under gravity, it detaches in form of a cold jet toward the base wall where it is reheated to repeat the process. As shown in Fig. 7, a cell is formed in between a thermal plume and a cold jet. Therefore, the arrangement of the plumes and jets coordinates with the cell structure in Fig. 3. The same thermal field pattern is observed in all the roofs. However, while there are thirteen plumes in the A-frame roof, there are only ten in the cathedral and barrel-vault roofs. The high number of cells in the A-frame roof encourages more uniform temperature across it.

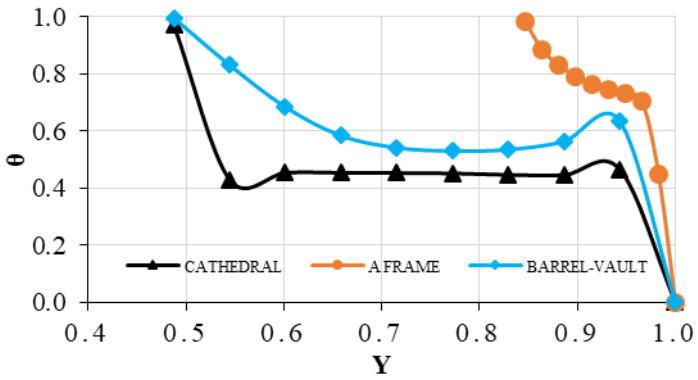

Fig. 8. Temperature variation along vertical midsections of the roofs.

The variation of air temperature along vertical cross-sectional lines at the midsections of the roofs is presented in Fig. 8. The line passes through the largest cell at the middle of the cathedral roof to show thermal boundary layer enclosing a quasi-isothermal core. In the A-frame and barrel-vault roofs, the line shows the variation of temperature along a plume rising from the hot ceiling to hit the upper vertex. The plot indicates that the midsection of the A-frame roof remains comparatively hotter than in other roofs. In the cathedral and barrel-vault roofs, temperature at the core of the cell is somewhat stable at the mean of the boundary temperatures.

3.4 Heat Transfer

The thermal performance of a roof indicates its ability to minimize the inflow of heat through the bounding walls. The pattern of heat transfer to and from the walls of the three roofs is illustrated in Fig. 9 by the spatial plots of the variation of the local Nusselt number along the hot base ceiling and the cold inclined walls for each of the roofs. The crest corresponds to a location where a hot plume rising from the base wall hits a cold inclined wall and a cold jet drops on the hot ceiling thereby maximizing heat exchange. The trough indicates the point at which a hot plume and a cold jet detach from the hot ceiling and a cold inclined wall respectively; indicating a near-zero thermal gradient condition. In major part of the length of the walls, the crest and trough variation is sequential; in synchronous with the formation of the plumes and jets in Fig. 7. The gap between a trough or crest on the ceiling and another on the upper wall forms the width of a cell. The heat exchange is relatively more uniform in the A-frame roof than in the other roofs. The nearer the hot and cold walls are to each other, the higher the heat transfer. In the case being considered in this study, the heat loss to the attic through the ceiling is least in the cathedral roof and highest in the barrel-vault roof.

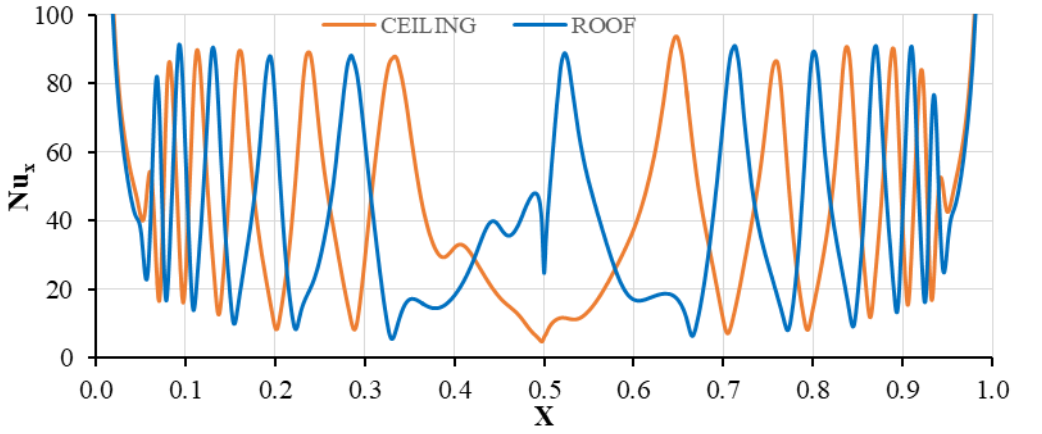

Cathedral

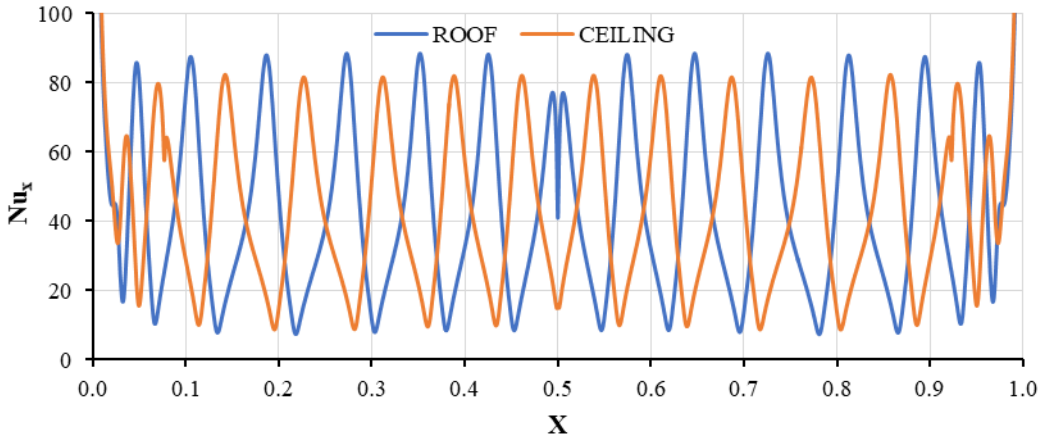

A-frame

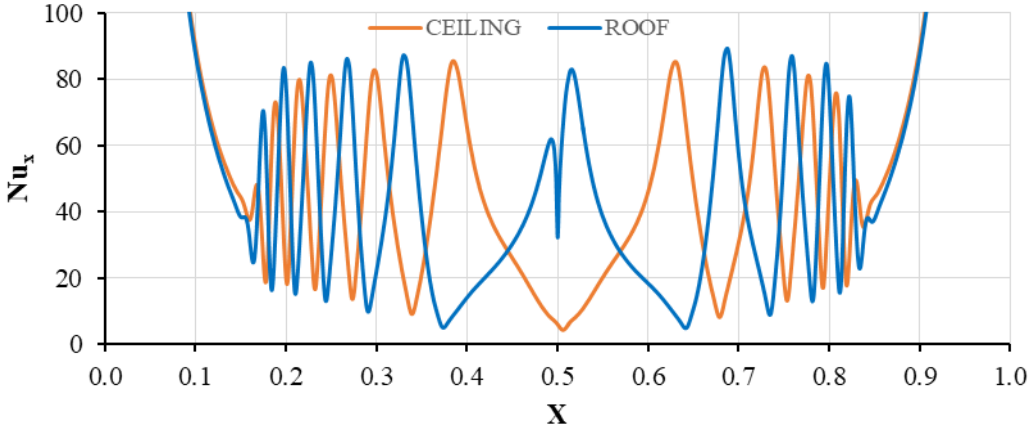

Barrel-vault

Fig. 9. Local Nusselt number variation along the hot ceiling and cold inclined walls for each enclosure.

Fig. 10 shows the mean Nusselt number which defines the overall heat loss through the hot ceiling into the attic of each roof. As shown in the figure, the mean Nusselt number is highest when the Barrel-vault shape is used for the ceiling while it is least when the cathedral shape is

used. This implies that the cathedral ceiling shape would minimize heat loss to the attic compared to the other ceiling shapes. Therefore, the cathedral roof has the best thermal performance.

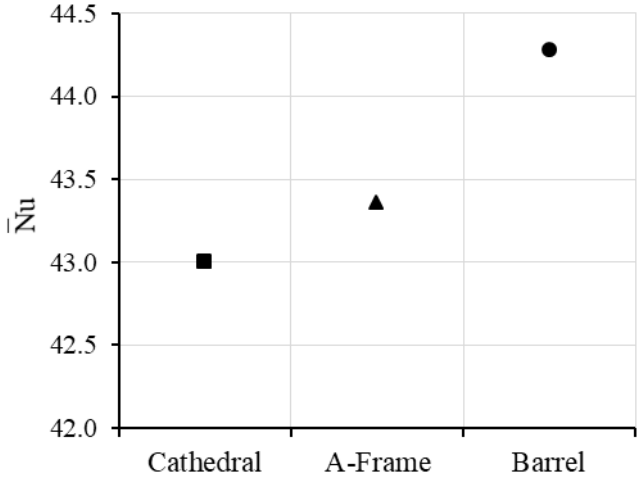

Fig. 10. Mean Nusselt number for the hot ceiling of the roofs.

4. CONCLUSIONS

A study on the effect of ceiling shape on the thermal performance of pitch roofs under winter condition has been investigated numerically. Three different ceiling shapes with special features, viz., cathedral, barrel-vault and A-frame, at the same 18^0 pitch angle and ceiling material are considered. The results obtained show that, in all roofs, multicellular flow fields are observed with the A-frame roof having the highest number of counter-rotating cells. The rotating speed of the cell is uniformly high across the A-frame roof but reduces from the midsection to the bottom corners in the roofs with cathedral and barrel-vault ceilings. The high number of recirculating cells across the roofs encourages uniform temperature distribution within the attics. Pressure is highest near the bottom corners and lowest around the upper vertex. While heat transfer along the ceiling is uniform in the A-frame roof, it is low at the midsection and high near the bottom corners of the cathedral and barrel-vault roofs. The mean Nusselt number is highest when the barrel-vault ceiling is used and lowest for the cathedral ceiling. Hence, the cathedral roof has the best thermal performance. The results also show generally that the A-frame roof with uniform heat and flow field require uniform insulation thickness along the ceiling to control heat exchange between the attic and the space below it. On the other hand, for the cathedral and the barrel-vault roofs, insulation thickness should increase gradually from the midsection to the bottom corners.

6. REFERENCES

Alencastro, J. Fuertes, A., Wilde, P. (2018) 'The relationship between quality defects and the thermal performance of buildings'. Renewable and Sustainable Energy Reviews, 81(1), 883-894.

Al-Sanea, S. A. (2002) 'Thermal performance of building roof elements'. Building and Environment, 37(7), 665-675.

Cui, H., Xu, F., Sahad, S. and Liu, Q., (2019) 'Transient free convection heat transfer in a section triangular prismatic enclosure with different aspect ratios', International Journal of Thermal Sciences, 139, 282-291.

Elnokaly, A., Ayoub, M. and Elseragy, A., (2019) 'Parametric investigation of traditional vaulted roofs in hot-arid climates', Renewable Energy, 138, 250-262.

Kamiyo, O. M., Angeli, D., Barozzi, G. S., Collins, M. W., Olunloyo, V. O. S., and Talabi, S. O. (2010) 'A comprehensive review of natural convection in triangular enclosures'. Applied Mechanics Reviews, 63(6), 060801.

Kamiyo, O., (2020) 'Numerical simulation of natural convection for raised-ceiling rooftop heated from below', Kufa Journal of Engineering, 11(4), 58-71

Kamiyo, O., (2021) 'Numerical study of natural convective heat transfer within M-shaped roofs', Kufa Journal of Engineering, 12(1), 95-110.

Kent, E. F. (2009a) 'Numerical analysis of laminar natural convection in isosceles triangular enclosures'. Proceedings of the Institution of Mechanical Engineers, Part C: Journal of Mechanical Engineering Science, 223(5), 1157-1169.

Kent, E. F. (2009b) 'Numerical analysis of laminar natural convection in isosceles triangular enclosures for cold base and hot inclined walls'. Mechanics Research Communications, 36(4), 497-508.

Koca, A. O. (2007) 'Natural convection heat transfer in a saltbox roof with eave in winter day conditions'. Proceedings of 9th REHVA World Congress: Clima 2007 "WellBeing Indoors", Helsinki, Finland. On CD.

Koca, A. O. (2008) 'Numerical analysis of natural convection in shed roofs with eave of buildings for cold climates'. Computers & Mathematics with Applications, 56(12), 3165-3174.

Oztop, H. F. (2007) 'Laminar natural convection heat transfer in a shed roof with or without eave for summer season'. Applied Thermal Engineering, 27(13), 2252-2265.

Oztop, H. F. (2012) 'Experimental and numerical analysis of buoyancy-induced flow in inclined triangular enclosures'. International Communications in Heat and Mass Transfer, 39(8), 1237-1244.

Penot, F., and N'Dame, A. (1992) 'Successive bifurcations of natural convection in a vertical enclosure heated from the side', Heat Transfer: Proceedings of the 3rd UK National Conference and First European Conference on Thermal Sciences, Birmingham, UK, 1, 507-513.

Raj, R., Pradyumna, K. C., Rakshith, B.R., Nithin, R.B. and Karthik, S.R., (2018) 'Combined natural convection and surface radiation inside vented triangular enclosure- an experimental study', International Conference on Research in Mechanical Engineering Sciences, 144, 04019.

Ridouane, E. H., Campo, A. and McGarry, M., (2005) 'Numerical computation of buoyant airflows confined to attic spaces under opposing hot and cold wall conditions, *International Journal of* Thermal Sciences. 44, 944–952.

Varol, Y. K. (2007) 'Effects of geometrical shape of roofs on natural convection for winter conditions'. Proceedings of 9th REHVA World Congress: Clima 2007 "WellBeing Indoors", Helsinki, Finland. On CD.

Varol, Y. K. (2007) 'Natural convection heat transfer in gambrel roofs'. Building and Environment, 42(3), 1291-1297.

Yesiloz, G. and Aydin, O., (2011) 'Natural convection in an inclined quadrantal cavity heated and cooled on adjacent walls'. Experimental Thermal and Fluid Science, 35, 1169–1176.

Yilmaz, Z., (2007) 'Evaluation of energy efficient design strategies for different climatic zones: Comparison of thermal performance of buildings in temperate-humid and hot-dry climate' Energy and Buildings, 39(3), 306-316.

Zhai, H. X. (2018) 'Natural convection and heat transfer on a section-triangular roof'. International Communications in Heat and Mass Transfer, 92, 23-30.